Pharmacological Research 152 (2020) 104586

Contents lists available at ScienceDirect

Pharmacological Research

journal homepage: www.elsevier.com/locate/yphrs

Apigenin inhibits STAT3/CD36 signaling axis and reduces visceral obesity

Tao Su[a,1], Chunhua Huang[b,1], Chunfang Yang[a], Ting Jiang[a], Junfang Su[a], Minting Chen[b], Sarwat Fatima[b], Ruihong Gong[b], Xianjing Hu[b], Zhaoxiang Bian[b,*], Zhongqiu Liu[a,**], Hiu Yee Kwan[b,*]

[a] International Institute for Translational Chinese Medicine, Guangzhou University of Chinese Medicine, Guangzhou, Guangdong, 510006, China
[b] Centre for Cancer and Inflammation Research, School of Chinese Medicine, Hong Kong Baptist University, Hong Kong, China

ARTICLE INFO

Keywords:
Apigenin
Visceral obesity
High fat diet
Signal transducer and activator of transcription 3
Cluster of differentiation 36

ABSTRACT

Visceral obesity is the excess deposition of visceral fat within the abdominal cavity that surrounds vital organs. Visceral obesity is directly associated with metabolic syndrome, breast cancer and endometrial cancer. In visceral obese subjects, signal transducer and activator of the transcription 3 (STAT3) in adipocytes is constitutively active. In this study, we aimed to screen for dietary herbal compounds that possess anti-visceral obesity effect. Apigenin is abundant in fruits and vegetables. Our data show that apigenin significantly reduces body weight and visceral adipose tissue (VAT), but not subcutaneous (SAT) and epididymal adipose tissues (EAT), of the high fat diet (HFD)-induced obese mice. Mechanistic studies show that HFD increases STAT3 phosphorylation in VAT, but not in SAT and EAT. Further studies suggest that apigenin binds to non-phosphorylated STAT3, reduces STAT3 phosphorylation and transcriptional activity in VAT, and consequently reduces the expression of STAT3 target gene cluster of differentiation 36 (CD36). The reduced CD36 expression in adipocytes reduces the expression of peroxisome proliferator-activated receptor gamma (PPAR-γ) which is the critical nuclear factor in adipogenesis. Our data show that apigenin reduces CD36 and PPAR-γ expressions and inhibits adipocyte differentiation; overexpression of constitutive active STAT3 reverses the apigenin-inhibited adipogenesis. Taken together, our data suggest that apigenin inhibits adipogenesis *via* the STAT3/CD36 axis. Our study has delineated the mechanism of action underlying the anti-visceral obesity effect of apigenin, and provide scientific evidence to support the development of apigenin as anti-visceral obesity therapeutic agent.

1. Introduction

Obesity is defined as excess accumulation of adipose tissue in the body. The worldwide prevalence of obesity keeps increasing, more than 1.9 billion adults were overweight, in which 650 million were obese. Different fat depots have different impacts on human physiology or disease pathogenesis because they have unique gene signatures [1]. Regional distribution and accumulation of the adipose tissues are the important indicator for many diseases. Visceral fat (organ fat or intra-abdominal fat) refers to the fat stored within the abdominal cavity that surrounds vital organs, such as the mesenteric, epididymal white adipose tissue and perirenal fat. Abnormally high deposition of visceral adipose tissue (VAT) is known as visceral obesity [2]. Excess visceral fat accumulation is correlated with increased mortality and higher risk of developing metabolic syndrome, including glucose intolerance, hypertension, dyslipidemia and insulin resistance [2–5]. The physiological characteristics of visceral fat such as adipocyte size and number, responsiveness to lipolytic stimulation, lipid storage capacity and inflammatory cytokine production may contribute to the development of metabolic syndromes and cardiovascular diseases [6]. Recently, the term “visceral adiposity syndrome” emerges [7], which refers to these cardiometabolic complications associated with excess accumulation of

Abbreviations: STAT3, Signal transducer and activator of transcription 3; VAT, visceral adipose tissue; SAT, subcutaneous adipose tissue; EAT, epididymal adipose tissue; BAT, brown adipose tissue

* Corresponding authors at: School of Chinese Medicine, Hong Kong Baptist University, 7 Baptist University Road, Kowloon Tong, Hong Kong, China.
** Corresponding author at: International Institute for Translational Chinese Medicine, Guangzhou University of Chinese Medicine, Guangzhou, Guangdong, 510006, China.
E-mail addresses: sutao@gzucm.edu.cn (T. Su), IVAN7456@hkbu.edu.hk (C. Huang), gzyangchunfang@163.com (C. Yang), gztingjiang@126.com (T. Jiang), sujunfang@gzucm.edu.cn (J. Su), 18482309@life.hkbu.edu.hk (M. Chen), sarwat@hkbu.edu.hk (S. Fatima), gongruihong@hkbu.edu.hk (R. Gong), huxj2003@163.com (X. Hu), bzxiang@hkbu.edu, bzxiang@hkbu.edu.hk (Z. Bian), liuzq@gzucm.edu.cn (Z. Liu), hykwan@hkbu.edu.hk (H.Y. Kwan).
[1] These authors are equally contributed to this work.

https://doi.org/10.1016/j.phrs.2019.104586
Received 8 February 2019; Received in revised form 26 September 2019; Accepted 2 December 2019
Available online 23 December 2019

visceral fat. Besides, epidemiological studies also show that visceral obesity is a significant risk factor for breast cancer [8]; and is associated with poor outcome in endometrial cancer [9].

Visceral obesity is not only the result of adopting western life style but is also the consequences of aging-associated muscle loss and hormonal changes [6,10]. Consumption of daily food that can help to reduce visceral fat may be a pragmatic strategy to combat visceral obesity. Apigenin is a common nature compound. It is a flavonoid belongs to the flavone structure class. In natural sources, apigenin is present as apigenin-7-O-glucoside and various acylated derivatives [11]. Apigenin is abundant in our daily fruits and vegetables such as parsley, onions, oranges, chamomile and wheat. Based on the United States Department of Agriculture (USDA) data, the contents of apigenin in parsley, peppermint, thyme, annual saw thistle leaves reach 10 − 50 mg/100 g. Apigenin is also a constituent in red wine [12]. Another common source of apigenin is herbal tea chamomile prepared from the dried flowers from *Matricaria chamomilla*. Apigenin is not only a phytochemical in our daily food; it is also used in alternative medicine for the treatment of asthma, intransigent insomnia, Parkinson's disease, neuralgia and shingles [13]. Recent experimental studies suggest that apigenin possesses anti-cancer effects [14]; and may be developed as chemo-preventive or chemotherapeutic agent. Apigenin also has free-radical scavenging activity [15], anti-hyperglycemic effect [16], and it reduces adipogenic and lipolytic gene expressions in adipocytes [17]. However, the underlying mechanism of action has not been delineated.

Signal transducer and activator of transcription 3 (STAT3) signaling is constantly activated in the VAT of obese subjects [18], it is considered as a pathogenic factor of visceral obesity. Besides, increasing evidences suggest that elevated expression of cluster determinant 36 (CD36) protein is closely associated with obesity. Interestingly, CD36 deficiency attenuates the accumulation of visceral fat and the development of obesity in obese mice [19,20]. However, the functional role of STAT3/CD36 axis in obesity is not known.

Given the pathological roles of STAT3 and CD36 in visceral obesity, we aimed to screen for dietary compounds that possessed potent anti-visceral obesity effect by regulating STAT3 or the STAT3/CD36 axis in adipocytes. Our data will provide scientific evidence for the development of the herbal dietary compound into an anti-visceral obesity therapeutic agent.

2. Materials and methods

2.1. Animal handling

C57BL/6 (C57) mice (16–18 g)were purchased from Laboratory Animal Center of Sun Yat-sen University (License number: SCXK (Guangdong) 2016-0029; Guangzhou, China), and were kept in the animal facility in the SPF animal laboratory (License number: SYXK (GZ) 2019-0144) at International Institute for Translational Chinese Medicine, Guangzhou University of Chinese Medicine (Guangzhou, China). Animal experiments were approved by the Guangzhou University of Chinese Medicine Animal Care and Use Committee (Guangzhou, China), and conducted according to the ethical standards and national guidelines. All mice were randomly selected to have either control diet (D12450 J Research Diets), or high fat diet (D12762 Research Diets) which was used to induce obesity. Both diet and water were supplied *ad libitum*. After 10-week of dietary intervention, the established diet-induced obesity (DIO) mouse models were used for the experiments. These DIO mice were given either apigenin by subcutaneous injection of 15 mg/kg/day, 30 mg/kg/day or vehicle alone as control for 13 days. Behavioural changes, body weight and food intake of these mice were recorded every day.

2.2. Measure the concentration of apigenin in mouse serum

The concentration of apigenin in the serum of the mice was analyzed by LC-MS/MS which is equipped with a 5500 QTRAP system (Applied Biosystems/MDS Sciex, Foster City, CA, USA) and a Shimadzu LC-30A liquid chromatography system. Chromatographic separation was performed on ACQUITY UPLC HSS T3 1.8 μm (2.1 × 150 mm) column. The temperature was maintained at 40 ℃ and the sample injection volume was 5 μL. The mobile phase consisted of methanol (a) and 0.1% formic acid aqueous solution (b) with a gradient elution of 35–65% A at 0–1.5 min, 65% A at 1.5 − 6 min, 65–95% A at 6 − 8 min, 35% A at 8.1–9.0 min. The flow rate was set at 0.35 mL/min. The optimized mass transition ion-pair (*m/z*) for apigenin quantization was 269.0/117.0.

2.3. Dissecting adipose tissues and isolating pre-adipocytes from mice

Adipose tissues were dissected from the mice as described [21]. VAT was dissected from the fat pad surrounding the kidneys. Epididymal adipose tissue (EAT) was dissected from the fat pad over the epididymis. Subcutaneous adipose tissue (SAT) was dissected from the fat pad under the skin. Brown adipose tissue (BAT) was dissected in the interscapular area with any superficial white adipose removed. Preadipocytes were isolated with collagenase protocol [22]. Briefly, white adipose tissues were minced into small pieces and were digested in 0.1% Type II collagenase (Sigma) in PBS at 37 ˚C for 20 min under shaking. The resulting cell pellets were washed with PBS and re-suspended in DMEM culture medium, there were kept at 37 ˚C humidified incubator with 5% CO_2.

2.4. 3T3-L1 preadipocyte differentiation

3T3-L1 preadipocytes were induced to differentiate to mature white adipocytes with differentiation inducing medium containing 1 mM dexamethasone, 0.5 mM isobutylmethylxanthine and 1.67 mM insulin in DMEM (Dulbecco's Modified Eagle's medium) supplemented with 10% FBS for 4 days before switching to DMEM with only 10% FBS and 10 μg/ml insulin for an additional 3 days [21].

2.5. Oil Red-O staining

Lipids are stained by Oil Red O staining. To quantify the staining, Oil Red-O was extracted from the cells with isopropanol containing 4% Nonidet P-40. The optical density was then measured at a wavelength of 520 nm.

2.6. Western blot

Protein samples were separated onto SDS-PAGE before transferring onto nitrocellulose membranes (Bio-Rad). Then, the membranes were blocked with milk and incubated with corresponding antibodies (Santa Cruz or Cell Signalling) overnight at 4 ˚C. Antibody against STAT3, p-STAT3 (Y705), p-STAT3 (Y727), CD36, p-IGF-1R (Y1161) and GAPDH were purchased from Abcam or Cell Signalling Technology, USA. Corresponding secondary antibodies were added and signals were detected by ECL detection system (Amersham Biosciences).

2.7. Real time PCR

Total RNA was isolated using TRIzol reagent (Invitrogen). Reverse transcription was performed with oligo-dT using MMLV reverse transcriptase (Promega, USA). Quantitative real time PCR was carried out by monitoring the increase in fluorescence of SYBR green with the ViiA 7 Real Time PCR System (Applied Biosystems, USA). The primer sequences [23–25] for peroxisome proliferator-activated receptor gamma (PPARγ) forward: GCCCTTTGGTGACTTTATGGA, PPARγ reverse: GCA GCAGGTTGTCTTGGATG; CCAAT/enhancer binding proteins (CEBP-β) forward: AGCCCCTACCTGGAGCCGCTCGCG, CEBP-β reverse: GCGCA GGGCGAACGGGAAACCG; glyceraldehyde-3-phosphate dehydrogenase

(GAPDH) forward: GTTGTCTCCTGCGACTTCA, GAPDH reverse: GGTG GTCCAGGGTTTCTT. Each sample was amplified in triplicate. Data were analysed by relative quantitation using $\Delta\Delta C_t$ method and normalized to GAPDH.

2.8. Transient reporter assay

Mouse CD36 promoter (-1963/+120) reporter was kindly provided by Prof Jianhua Shao from the University of California [26]. HEK293 cells grown in 24-well plates were co-transfected with 0.5 μg of CD36 promoter reporter and 0.02 μg of pRLSV40 encoding Renilla luciferase (rLuc) (Promega). Control cells were co-transfected with 0.5ug empty pGL3-basic luciferase reporter vector and 0.02 μg pRL-SV40 encoding rLuc. At 48 h-post-transfection, cells were treated with apigenin for 24 h before dual-luciferase assay (Promega) was performed. The luciferase readings for each sample were normalized against the rLuc levels.

2.9. Transfection

The siRNA transfection was performed with Lipofectamine RNAiMAX transfection reagent (ThermoFisher Scientific). Negative control (NC) with non-sense sequence was used as control. We followed the company's protocol to do the transfection. Briefly, the RNA-RNAiMAX complexes were prepared with the recommended ratio in the Opti-MEM reduced serum medium and were added to the cells. Cells were then incubated for 2 days at 37 °C. STAT3C or CD36 transfection was performed with Lipofectamine 3000 transfection reagent (ThermoFisher Scientific). Empty vector (EV) was used as control. DNA-lipofectamine-3000 complexes were prepared with the recommended ratio and were added to the cells. Cells were then incubated in 37 °C humidified incubator with 5% CO_2 for 3 days.

2.10. Lipidomics analysis and data processing

Lipidomics study was done as described [27]. Briefly, we analysed the lipids with Agilent 6540 UHD Accurate-Mass Q-TOF LC/MS mass spectrometer (Agilent Technologies, USA) connected to an Agilent 1290 Infinity UHPLC. Agilent 6450 Triple Quadrupole LC/MS system connected to an Agilent 1290 Infinity UHPLC is used for specific quantification of targeted bioactive lipids and lipid metabolites [20]. Raw data were first processed by MassHunter Workstation software (Version B.04.00 Qualitative Analysis) and then analysed by Mass Profiler Professional (MPP) software (Version 2.2). Only entities with abundances above 3000cps were selected. These entities were then passed a tolerance window of 0.15 min and 2 m Da chosen for alignment of RT and *m/z* values, respectively. We employed one-way ANOVA to do the statistical analysis. The *p*-value of ANOVA was set at 0.05 that corresponds to the significance level of 95%.

2.11. Molecular docking

The binding mode between apigenin and STAT3 was investigated using Autodock vina 1.1.2. Three-dimensional (3D) structure of STAT3 was downloaded from RCSB Protein Data Bank (http://www.rcsb.org/pdb), and the 3D structure of apigenin was drawn by ChemBioDraw Ultra 14.0 and ChemBio3D Ultra 14.0 software. AutoDockTools 1.5.6 package was used to generate the docking input files.

2.12. Molecular dynamics

Molecular dynamics simulation was performed using AmberTools 14 software. General AMBER force field (GAFF) parameters were assigned to the ligands, and the partial charges were calculated using the AM1-BCC method. The ff14SB force field was used for the protein. The STAT3-apigenin complex was charge-neutralized by adding sodium counterions and was then surrounded by a periodic box of TIP3P water molecules extending up to 10 Å from the solute. First, energy minimizations using the steepest descent method, followed by the conjugate gradient method, were performed for each system. Each system was gradually heated from 0 to 300 K within 50 ps, followed by a further 50 ps of equilibration at 300 K to obtain a stable density. An unconstrained production phase was initiated and continued for 100 ns in a NPT ensemble at 1 atm and 300 K. During the simulations, the long-range electrostatic interactions were evaluated by the particle mesh Ewald (PME) algorithm. The cut off distance for the long-range van der Waals interaction was set to 10 Å. The SHAKE method was applied to constrain the bond lengths of hydrogen atoms attached to heteroatoms. The time step used for the molecular dynamics simulations was set to 2.0 fs, and the trajectory files were collected every 20 ps for the subsequent analysis. Interaction between apigenin and each residue was computed using the MM/GBSA decomposition process by the mm_pbsa program in AmberTools 14. The binding interaction of apigenin-residue pair includes three energy terms: van der Waals contribution (vdw), electrostatic contribution (ele), the polar solvation contribution (polar E) and nonpolar solvation contribution (nonpolar E). All energy components were calculated using the 50 snapshots extracted from the molecular dynamics trajectory from 50 to 100 ns.

2.13. Thermal shift assay

The temperature-dependent thermal shift assay was performed as described [28]. Briefly, 3T3-L1 cell lysate was incubated with 100 μM of apigenin at each temperature set point for 4 min. The samples were centrifuged at 4 °C. The supernatant was mixed with loading buffer and separated on SDS-PAGE for immunoblotting analysis of STAT3.

2.14. Hematoxylin and eosin staining for VAT

VAT were fixed in 4% paraformaldehyde, embedded in paraffin, and then sliced at 4 μm thickness. The slices were stained with hematoxylin and eosin, and examined by light microscopy.

2.15. Statistical analysis

Results were shown as mean ± SEM. Data were analyzed by one-way ANOVA followed by the Dunnett's multiple comparisons. Statistical analyses were carried out using GraphPad Prism (GraphPad Software, San Diego, CA, USA) version 7.0. $p < 0.05$ was considered statistically significant.

3. Results

3.1. Apigenin treatment significantly reduces body weight and VAT of the DIO mice

We first established DIO mouse model by feeding male C57 mice with high fat diet (#D12492 Research Diets) for 10 weeks. Mice in control group had a comparable control diet (CD) (#D12450 J Research Diets). As shown in Fig. 1A, body weights of the mice in HFD group were significantly higher than those in CD group. The increase in body weight may due to the significant increase in the white adipose tissues such as VAT (Fig. 1B) and EAT (Fig. 1D), and to a less extend in SAT (Fig. 1C). However, the mass of BAT was not affected by the dietary intervention (Fig. 1E).

To investigate the anti-obesity effects of apigenin (Fig. 1F), we treated the DIO mice with two different dosages of apigenin, respectively. Fig. 1G showed the detailed treatment timeline. We found that both dosages significantly reduced the body weight of DIO mice after 13 days of treatment (Fig. 1H). The decrease in body weight is not due to the reduction in the major organ weight (supplementary Fig S1). The treatment significantly reduced the mass of VAT (Fig. 1I) and the visceral adipocyte sizes of the DIO mice (Fig. 1J). Interestingly,

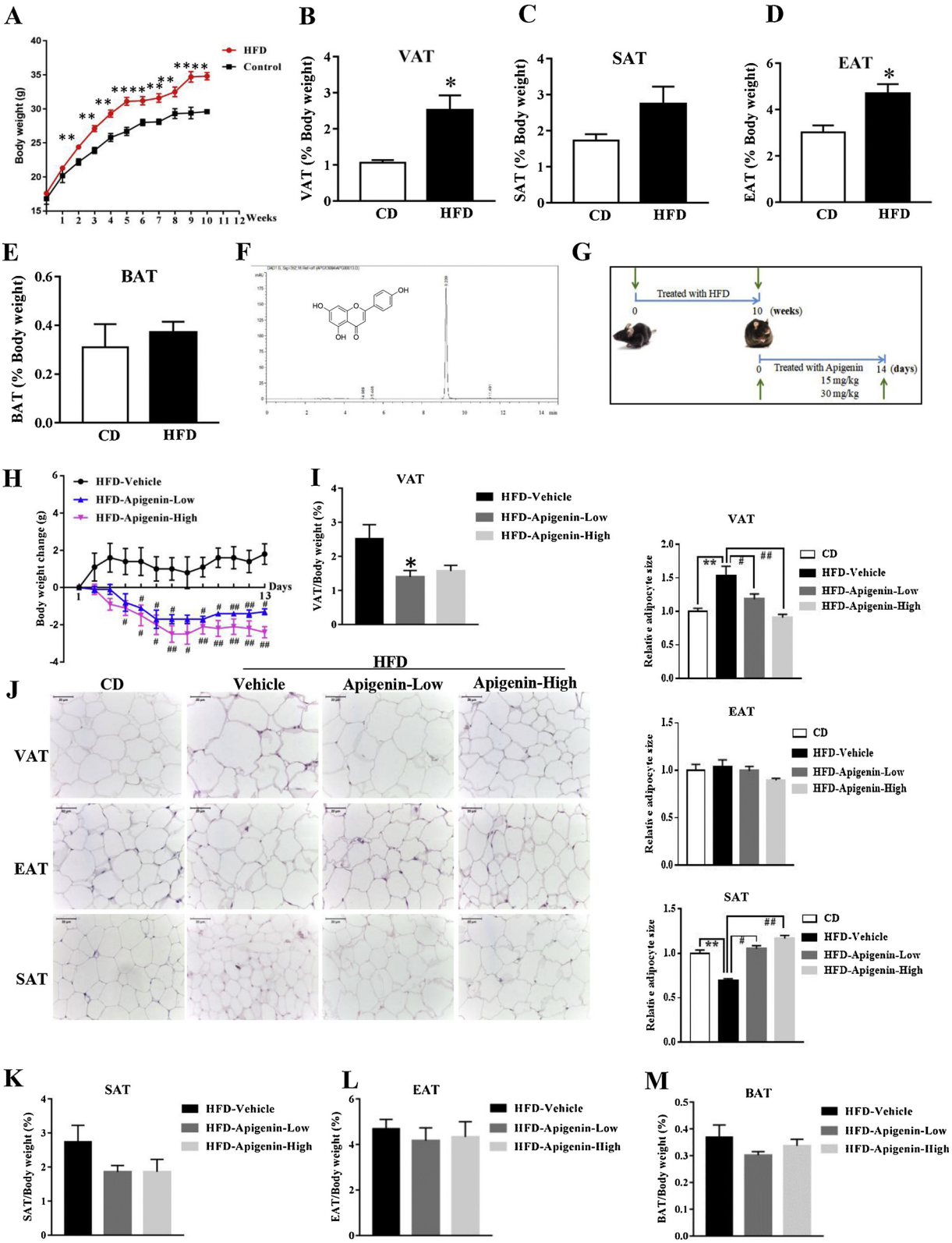

Fig. 1. High fat diet (HFD) significantly increased (A) body weight, the mass of (B) VAT and (D) EAT, and to a lesser extend the mass of (C) SAT. The dietary intervention did not affect the mass of (E) BAT. (F) Apigenin was used for the treatment, and (G) the treatment schedule. Apigenin significantly reduced (H) body weight of the diet-induced obesity (DIO) mice, and also (I–J) VAT, but not (K) SAT, (L) EAT and (M) BAT of the mice. Shown are the mean ± SEM, 6 mice in each group. $^{*}p < 0.05$, $^{**}p < 0.01$, *vs.* CD; $^{\#}p < 0.05$, $^{\#\#}p < 0.01$, *vs.* HFD-vehicle, as indicated. VAT, visceral adipose tissue; SAT, subcutaneous adipose tissue; EAT, epididymal adipose tissue; BAT, brown adipose tissue.

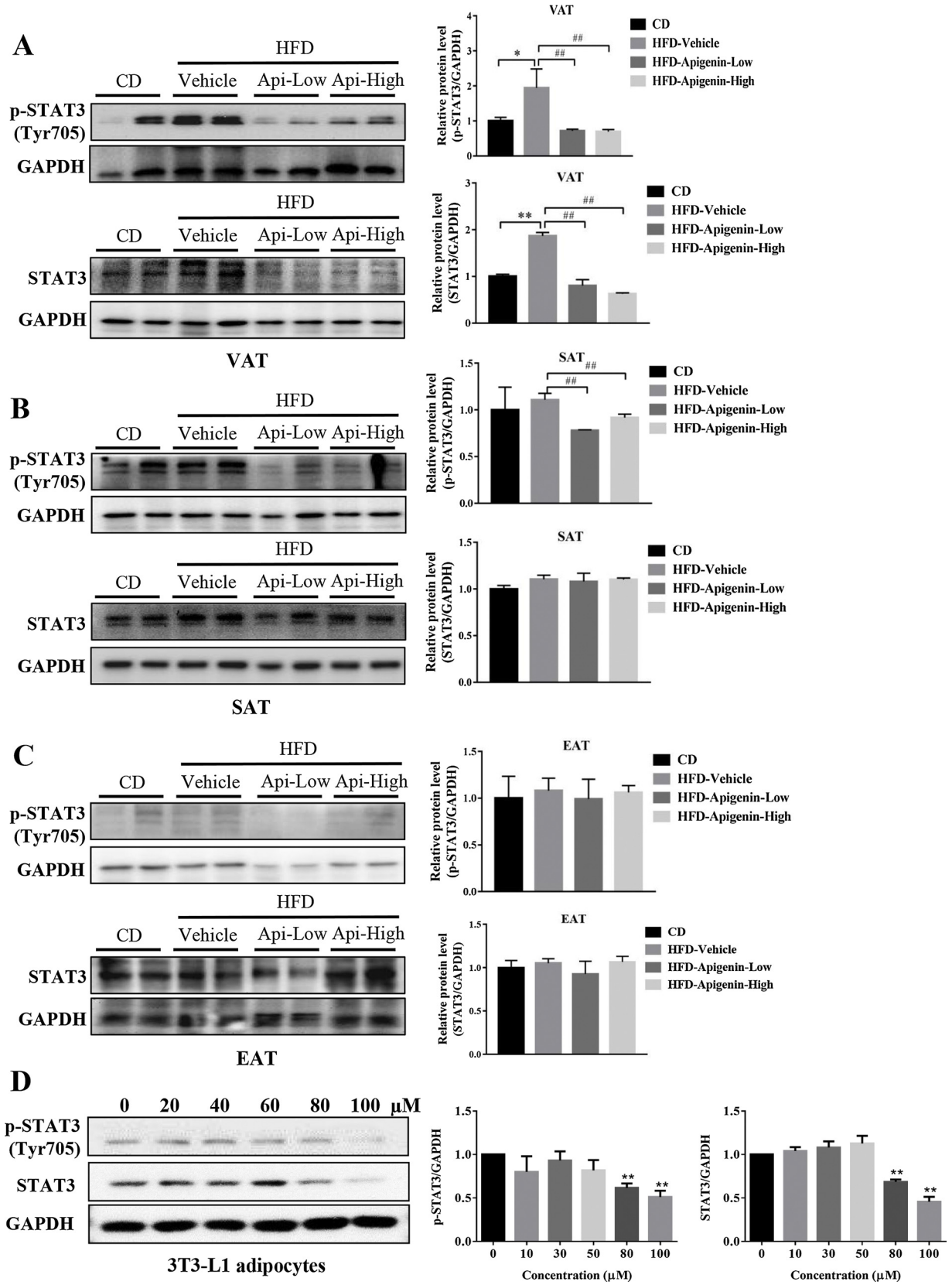

Fig. 2. Apigenin significantly reduced STAT3 phosphorylation (Tyr705) in (A) VAT, and to a lesser extend in (B) SAT, but not in (C) EAT of the DIO mice. Apigenin also significantly reduced STAT3 protein expressions in (A) VAT, but not in (B) SAT and (C) EAT of the DIO mice. Shown are the mean ± SEM, 6 mice in each group. $^{*}p < 0.05$, $^{**}p < 0.01$ *vs.* CD, $^{\#\#}p < 0.01$, *vs.* HFD-vehicle, as indicated. (D) Apigenin reduced STAT3 protein expression and STAT3 phosphorylation (Tyr705) in 3T3-L1 adipocytes. Shown are the mean ± SEM, n = 3 individual experiments. $^{*}p < 0.05$, $^{**}p < 0.01$, *vs.* control. VAT, visceral adipose tissue; SAT, subcutaneous adipose tissue; EAT, epididymal adipose tissue.

apigenin treatment did not significantly affect the mass of SAT (Fig. 1K), EAT (Fig. 1L) and BAT (Fig. 1M).

We also examined the serum levels of apigenin in these mice. We found that the concentration of apigenin was 40.6 ± 6.8 ng/mL in low-dosage group, and 95.2 ± 12.5 ng/mL in high-dosage group. The representative chromatograms were shown in the supplementary Fig S2.

3.2. Apigenin treatment reverses the HFD-increased STAT3 phosphorylation in VAT in DIO mice

To investigate how apigenin reduced VAT in DIO mice, we performed a high-throughput screening of the lipogenic signalling pathways that were affected by the apigenin treatment. STAT3 has been reported to promote adipogenesis [29]. Interestingly, we found that HFD feeding increased STAT3 phosphorylation in VAT (Fig. 2A), but not in SAT (Fig. 2B) and EAT (Fig. 2C). Apigenin treatment significantly reduced the HFD-increased STAT3 phosphorylation (Tyr705) in VAT (Fig. 2A), and to a less extend in SAT (Fig. 2B) and EAT (Fig. 2C). The inhibitory effect of apigenin on STAT3 phosphorylation was further suggested in cell model, in which apigenin reduced STAT3 phosphorylation (Tyr705) in 3T3-L1 adipocytes in a dose-dependent manner (Fig. 2D). Apigenin also reduced STAT3 protein levels in 3T3-L1 cells (Fig. 2D) and VAT (Fig. 2A) of the DIO mice, but not in SAT (Fig. 2B) and EAT (Fig. 2C).

3.3. Apigenin binds to non-phosphorylated STAT3 and inhibits its activity

Next, we examined how apigenin affected STAT3 phosphorylation. We first examined whether apigenin affected the upstream signalling molecules in the STAT3 signalling pathway. Study suggests that STAT3 is activated upon insulin-like growth factor 1 receptor (IGF-1R) activation in the adipose tissue in obese subjects [30]. However, we found that apigenin did not affect IGF-1R phosphorylation in VAT (Fig. 3A), SAT (Fig. 3B) and EAT (Fig. 3C), suggesting that IGF-1R may not be involved in the inhibitory effect.

To explore whether apigenin binds to the non-phosphorylated STAT3, we performed molecular docking experiments with Auodock vina 1.1.2. STAT3 inhibitor WP1066 served as positive control. The binding energy of apigenin and WP1099 to STAT3 were -8.9 and -7.4 kcal/mol, respectively. The three-dimensional ribbon model of the apigenin-STAT3 and WP1066-STAT3 complex were showed in Fig. 3D and 3E, respectively. We found that hydrogen bond was formed between the backbone of Arg247 in STAT3 subunit A and apigenin, and the donor-acceptor distance was 3.0 Å. To explore the dynamic stability of the model and to ensure the rationality of the sampling strategy, we performed molecular dynamic with AmberTools 14 software, and calculated the root-mean-square deviation (RMSD) values of the protein backbone based on the starting structure along the simulation time. As shown in Fig. 3F, the system was stable during the simulation. The RMSD of apigenin bound to STAT3 proteins was around 5 Å during the 100 ns MD simulation. The surface presentation of the apigenin-STAT3 complexes at 0 ns and 100 ns were shown in Fig. 3G and H, respectively. These molecular simulation results suggest that apigenin directly binds to non-phosphorylated STAT3 protein and changes its conformation and activity.

The binding between apigenin and STAT3 protein is further suggested by cellular thermal shift assay which is a reliable ligand-binding assay to show whether the small molecule acts on the protein of interest [31]. Data showed that apigenin increases the thermal stability of STAT3 in 3T3-L1 cell lysates as measured by the temperature-dependent cellular thermal shift assay (Fig. 3I). These data suggest that apigenin binds to STAT3, and hence increases the thermal stability of STAT3.

3.4. Apigenin reduces expression of STAT3 downstream target CD36 in adipocytes

Since STAT3 is a transcription factor, we next investigated the downstream target gene of STAT3 that mediated the anti-obesity effect of apigenin. When we overexpressed constitutive active STAT3 in HEK293 cell model (Fig. 4A), we found that CD36 expression was significantly elevated (Fig. 4B). Our data agree with a recent study suggesting that CD36 is a downstream target of STAT3 [32]. We next examined whether apigenin affected CD36 promoter activity in adipocytes. We overexpressed a mouse CD36 promoter -1963/+120 [26] in the 3T3-L1 pre-adipocytes, and we treated these cells with apigenin. We found that apigenin significantly reduced the activity of the mouse CD36 promoter (Fig. 4C), and expressions of CD36 mRNA (Fig. 4D) and protein (Fig. 4E) in the 3T3-L1 cells. In the DIO mouse model, apigenin also significantly reduced CD36 expressions in the white adipose tissues (Fig. 4F–H).

CD36 is a fatty acid translocase protein that facilitates fatty acid uptake in various cell types [33]. The reduced expression of CD36 in adipocytes should affect the lipid profiles in the adipocytes. Therefore, we performed lipidomics to examine whether the lipid profiles in the adipocytes were changed after the treatment. We found that the lipid samples of the control and apigenin-treated 3T3-L1 cells showed distinct clustering (Fig. 4I), suggesting the apigenin-treated cells have a lipidomics profiles different from that of the control cells. Furthermore, the free fatty acid levels in the apigenin-treated 3T3-L1 cells were less than that of the control cells (Fig. 4J). In DIO mouse model, the lipid samples of the VAT dissected from control mice and apigenin-treated mice also showed distinct clustering (Fig. 4K). Fig. 4L shows the regulatory networks of the highlighted fatty acids that had significantly difference between the VAT of the control DIO mice and apigenin-treated DIO mice.

3.5. Reduction of CD36 expression by apigenin inhibits adipocyte differentiation

Next, we investigated whether CD36 plays a role in adipogenesis. We found that after CD36 was knockout in 3T3-L1 pre-adipocytes (Fig. 5A), the expression of PPARγ was significantly reduced (Fig. 5B), suggesting CD36 regulates PPARγ expression in the adipocytes. Interestingly, apigenin treatment also significantly reduced PPARγ expression in 3T3-L1 adipocytes *in vitro* (Fig. 5C) and in *ex vivo* model with pre-adipocytes isolated from mouse (Fig. 5D).

Next, we examined whether STAT3/CD36 axis was involved in the inhibitory effect of apigenin. As shown in Fig. 5E and F, apigenin inhibited adipocyte differentiation. Knockout of STAT3 significantly reduced adipogenesis (Fig. 5G and H). Overexpression of constitutive active STAT3 (Stat3C) reversed the apigenin-reduced adipogenesis (Fig. 5I and J), suggesting STAT3 activity is involved in the apigenin-reduced adipogenesis.

4. Discussion

Our study suggests that apigenin possesses anti-visceral obesity effect because it significantly reduces body weight and VAT of the DIO mice. Interestingly, HFD increases STAT3 phosphorylation in VAT, which is reversed by apigenin. The subsequent reduction of STAT3 target gene CD36 inhibited pre-adipocyte differentiation.

Signal transducer and activator of transcription 3 (STAT3) is a transcription factor and its expression is upregulated during adipocyte differentiation [34]. Activation of the Janus kinase (JAK)/STAT3 axis promotes pre-adipocyte differentiation by modulating mitotic clonal expansion [29] which is a proliferative phase that occurs after induction of adipogenesis in 3T3-L1 cell model. However, adipocyte differentiation is a complex process that involves many transcription factors and nuclear receptors. PPARγ is the most critical nuclear receptor that

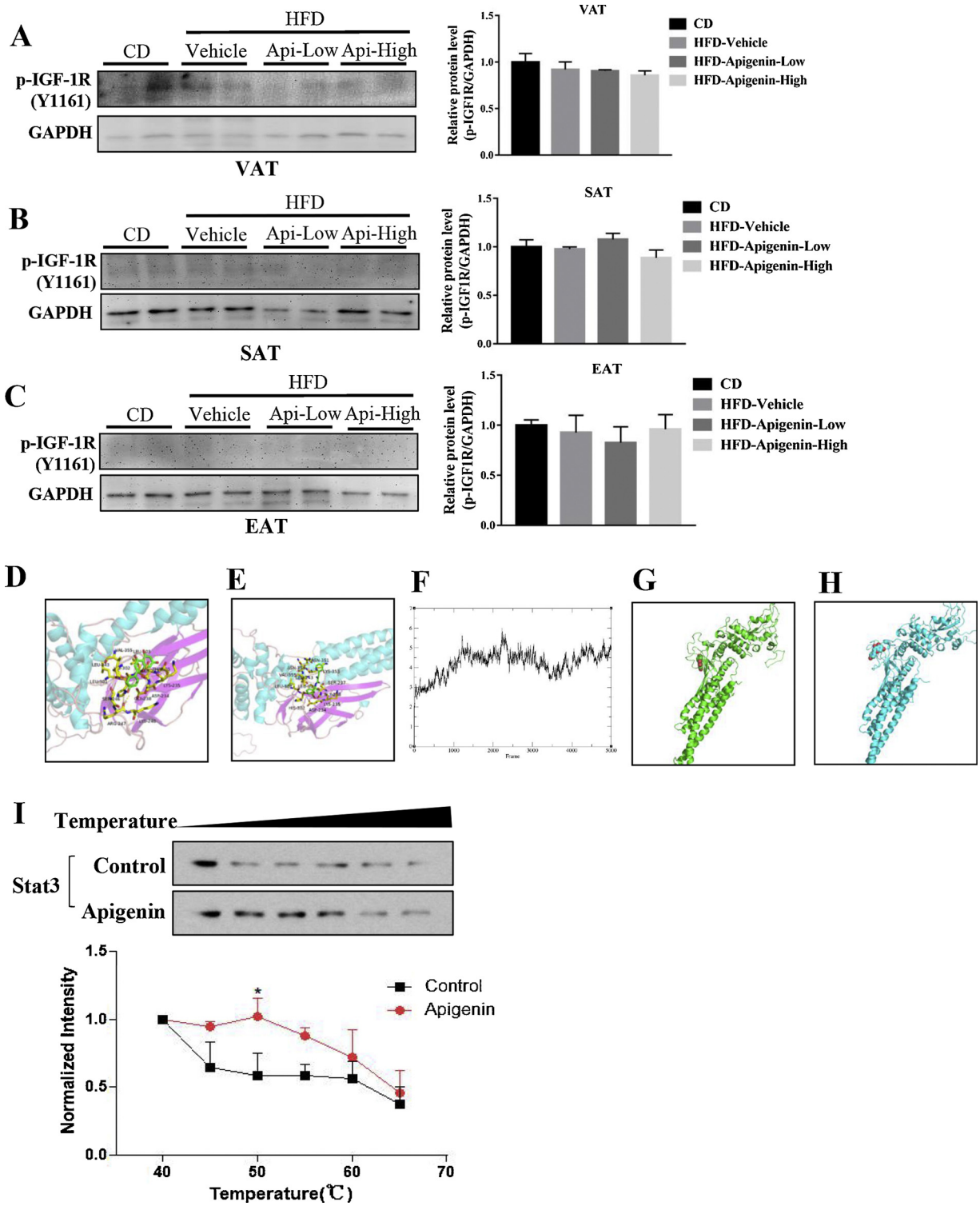

Fig. 3. Apigenin did not affect the phosphorylation of insulin growth factor receptor 1 (IGF-1R) (Y1161) in (A) VAT, (B) SAT and (C) EAT of the DIO mice. Shown are the mean ± SEM, 6 mice in each group. VAT, visceral adipose tissue; SAT, subcutaneous adipose tissue; EAT, epididymal adipose tissue. The binding of apigenin with STAT3 is suggested by (D–E) three-dimensional ribbon model of apigenin in complex with STAT3; (F) the plots of root mean square deviation (RMSD) of heavy atoms of unphosphorylated STAT3; (G–H) formation of the apigenin-unphosphorylated STAT3 complexes at 0 ns and 100 ns, respectively. (I) Temperature-dependent cellular thermal shift assay with 3T3-L1 cell lysate and apigenin at 100 μM. Shown are the mean ± SEM, n = 3 individual experiments. *$p < 0.05$, *vs.* control.

promotes adipocyte differentiation. Wang et al. suggests that STAT3 regulates adipocyte differentiation *via* PPARγ because PPARγ agonist abolished the STAT3-inhibitor- and RNAi (RNA interference)-mediated suppression of adipogenesis [35]. However, this experimental design cannot clearly elucidate PPARγ is a direct downstream target of STAT3 because PPARγ is a master regulator of adipogenesis in the late stage of adipocyte differentiation. Overexpression of PPARγ or activation of PPARγ with agonist *per se*, will regulate expressions of many target genes that are responsible for the establishment of the mature adipocyte phenotypes such as increasing lipid accumulation and insulin

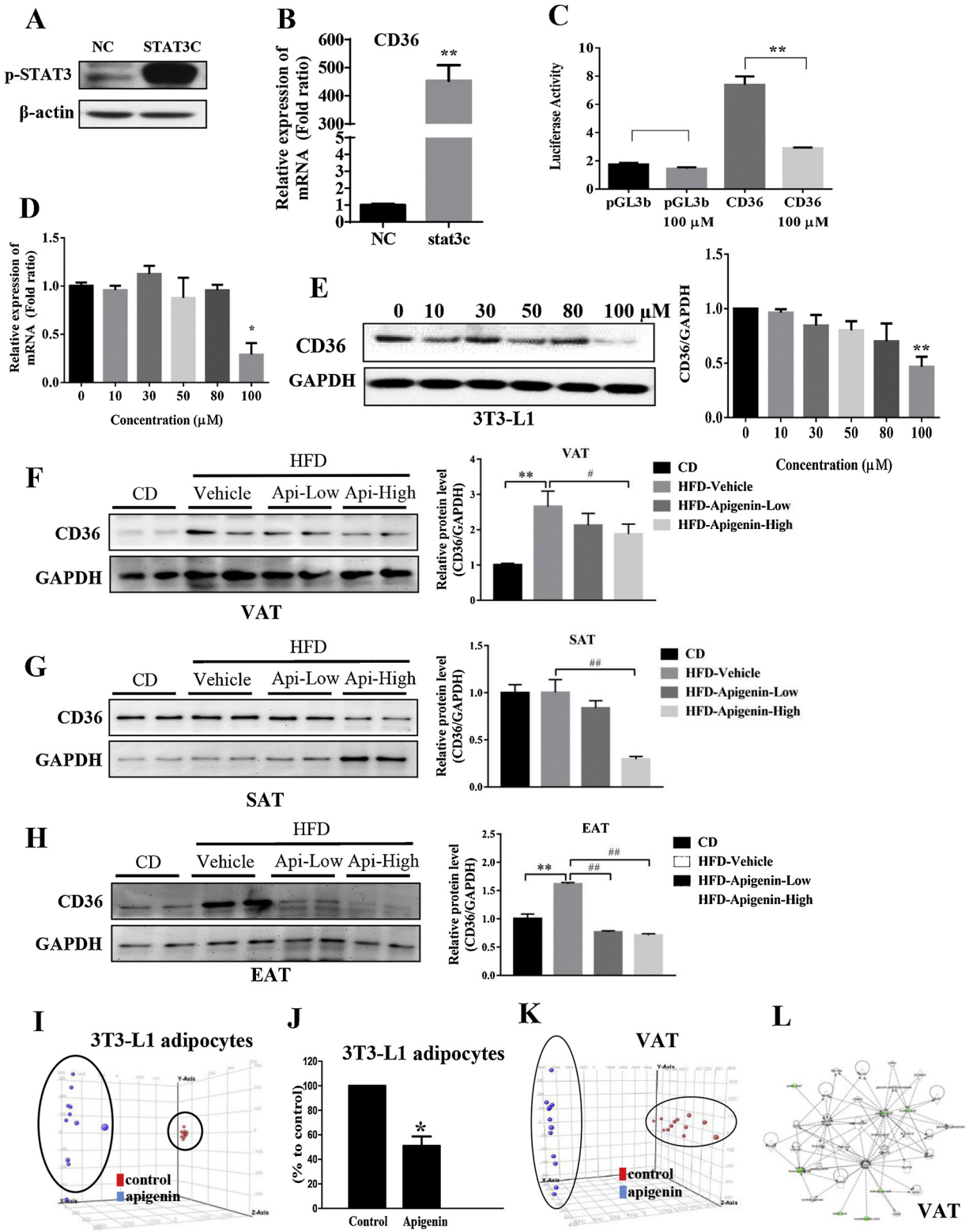

Fig. 4. (A) Overexpression of constitutive active STAT3C in HEK293 cell model, and (B) the expression level of CD36 mRNA in the STAT3C-overexpressed cells. Apigenin reduced (C) mouse CD36 promoter (−1963/+120) activity, (D) CD36 mRNA and (E) CD36 protein levels in 3T3-L1 adipocytes. Apigenin reduces CD36 protein expressions in (F) VAT, (G) SAT and (H) EAT of the DIO mice. (I) Principle component analysis of the lipid samples of control and apigenin-treated 3T3-L1 cells and (J) apigenin reduced free fatty acid levels of the 3T3-L1 cells. (K) Principle component analysis of the VAT of the DIO mouse model after apigenin treatment and (L) the regulatory networks of the highlighted fatty acids that showed significantly difference between the VAT of the control DIO mice and the apigenin-treated DIO mice. For A–E and J, shown are the mean ± SEM, n = 3 individual experiments. $^{*}p < 0.05$, $^{**}p < 0.01$ *vs.* NC or control, as indicated. For F–H, shown are the mean ± SEM. 6 mice in each group. $^{**}p < 0.01$, *vs.* CD; $^{\#}p < 0.05$, $^{\#\#}p < 0.01$, *vs.* HFD-vehicle, as indicated. VAT, visceral adipose tissue; SAT, subcutaneous adipose tissue; EAT, epididymal adipose tissue.

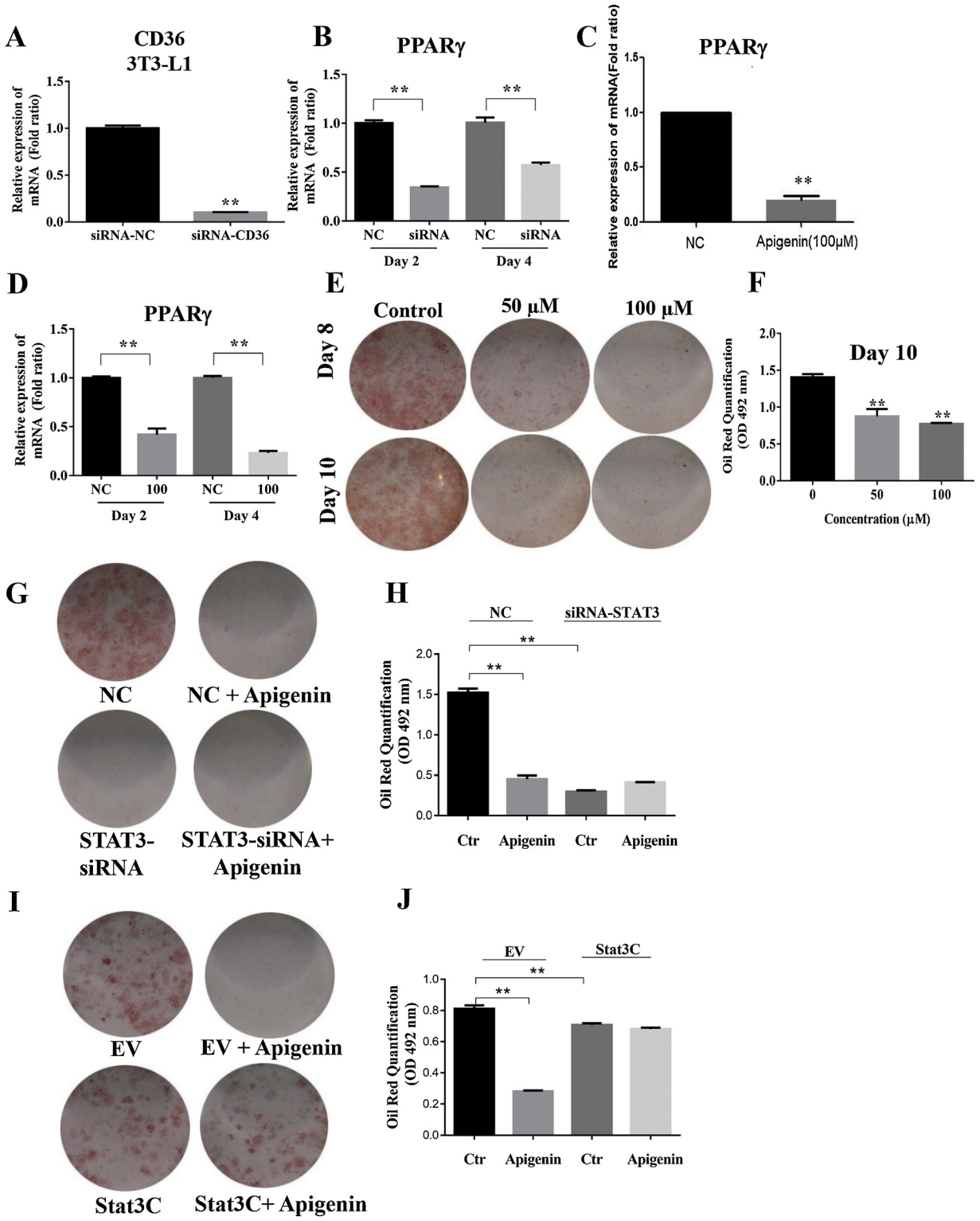

Fig. 5. (A) Expression of CD36 mRNA after siRNA-mediated knockout of CD36 in 3T3-L1 adipocytes; and (B) the expression of PPARγ in these CD36-knockout 3T3-L1 cells. Apigenin reduced PPARγ mRNA expressions in (C) 3T3-L1 adipocytes and (D) isolated mouse pre-adipocytes. (E) Differentiation of 3T3-L1 adipocytes in the presence or absence of apigenin at the indicated concentrations, and (F) quantification of Oil Red O staining on Day 10 of the differentiation. (G) Differentiation of 3T3-L1 pre-adipocytes transfected with siRNA-STAT3 or negative control (NC) in the presence or absence of apigenin (100 μM), and (H) quantification of corresponding Oil Red O staining. (I) Differentiation of 3T3-L1 pre-adipocytes overexpressed with constitutive active STAT3 (Stat3C) or empty vector (EV) in the presence or absence of apigenin (100 μM), and (J) quantification of the corresponding Oil Red O staining. Shown are the mean ± SEM, n = 3 individual experiments. $^{**}p < 0.01$ *vs.* siRNA-NC, NC or control, as indicated. (For interpretation of the references to colour in this figure legend, the reader is referred to the web version of this article).

sensitivity. Therefore, further study is needed to find out whether PPARγ is a direct downstream target gene of STAT3 that mediates the STAT3-enhanced adipocyte differentiation.

Our study shows that overexpression of constitutively active STAT3 significantly increases CD36 expression in HEK293 cell model, suggesting CD36 is a direct downstream target of STAT3. Our study also shows that HFD increases STAT3 phosphorylation in VAT. Inhibition of STAT3 activity and the subsequent reduction of CD36 expression in the adipocytes underlies the anti-visceral obesity of apigenin. Indeed, a recent study suggests that inhibition of CD36 reduces visceral fat accumulation in obese mice [36], and CD36 promotes adipogenesis [37]. CD36 also plays a role in metabolic disorders [38]. Studies show that plasma homocysteine and folate are related to the arterial blood pressure in type 2 diabetes mellitus [39]. Elevated level of homocysteine has also been reported in type 1 diabetes mellitus patients who have developed complications such as diabetic retinopathy and diabetic nephropathy [40]. It would be interesting to investigate whether CD36 regulates plasma homocysteine and folate levels in diabetic models and whether apigenin can be the therapeutics for diabetes *via* its regulation on CD36. Using apigenin as therapeutics for treatment will be beneficial to the patients especially those with type 1 diabetes because they do not need to perform pancreas transplantation [41,42].

Previous study shows that apigenin modulates PPARγ and regulates lipid metabolism in liver in Nrf2-dependent manner, in which apigenin activates PPARγ and the activation is inhibited by Nrf2 [43]. Another study shows that apigenin activates PPARγ and promotes the polarization of macrophages from M1 to M2 both *in vivo* and *in vitro* [44]. Here, our data show that apigenin reduces PPARγ expressions in adipocytes. The effect of apigenin on PPARγ seems to be cell specific. Furthermore, the interplay between PPARγ and CD36 is controversial. Previous study has suggested CD36 regulates PPARγ and modulate lipid metabolism in response to growth hormone releasing peptides [45]. However, another study has suggested that PPARγ expression induces CD36 expression in the vascular smooth muscle cells during the development of atherosclerosis [46]. Our data suggest that apigenin inhibits PPARγ activity in adipocyte, which is dependent upon CD36. Nevertheless, we cannot rule out the possibility that apigenin also has a direct effect on PPARγ expression independent of CD36 in our model.

Apigenin is a flavonoid with low oral bioactivity. Studies have reported that the oral bioavailability of flavonoid is less than 3% in rats [47]. Actually, not only apigenin, many flavonoid compounds, such as quercetin [48], baicalein [49] and luteolin [50] have the similar problem. There are two possible reasons for explaining the low bioavailability of the tested drugs, incomplete absorption and first-pass metabolism. Studies have demonstrated that the major reason of apigenin's low bioavailability is owing to its poor permeation across gastrointestinal epithelia [51]; others speculate that the ingested apigenin was rapidly metabolized after absorption, hence, it shows poor oral bioactivity [52]. For these reasons, in this study, we treated mice with subcutaneous injection but not oral administration. Actually, medication *via* subcutaneous injection has been reported in many studies [53,54].

5. Conclusion

The direct linkage or the causal relationship between visceral fat and metabolic syndrome is difficult to be elucidated due to considerable metabolic heterogeneity of the individuals. Nevertheless, the visceral fat is considered as a factor that exacerbates the individual genetic susceptibility to the metabolic syndrome and also exacerbates the complication of the metabolic syndrome. Our study has clearly demonstrated the anti-visceral obesity effect of apigenin; further clinical study is desperately needed to validate the effect. Apigenin is a natural compound and is commonly found in vegetables and fruits, development of apigenin as therapeutics or health product to control body weight will definitely benefit the mankind.

Declaration of Competing Interest

The authors declare that they have no competing interests,

Acknowledgements

This work was partially supported by Research Grant Council of HKSAR HKBU-22103017-ECS and Natural Science Foundation of Guangdong Province#2018A0303130122 to HYK; the National Natural Science Foundation of China81703705 and the Opening Project of Zhejiang Provincial Preponderant and Characteristic Subject of Key University (Traditional Chinese Pharmacology), Zhejiang Chinese Medical University (ZYAOX2018010) to ST; and the Guangdong Key Laboratory for translational Cancer research of Chinese Medicine (2018B030322011) to LZQ. We specially thank for Dr Sarwat Fatima for her editing of the manuscript.

Appendix A. Supplementary data

Supplementary material related to this article can be found, in the online version, at doi:https://doi.org/10.1016/j.phrs.2019.104586.

References

[1] Y. Yamamoto, S. Gesta, K.Y. Lee, T.T. Tran, P. Saadatirad, C.R. Kahn, Adipose depots possess unique developmental gene signatures, Obesity 18 (2010) 872–878.
[2] A. Shuster, M. Patlas, H.J. Pinthus, M. Mourtzakis, The clinical importance of visceral adiposity: a critical review of methods for visceral adipose tissue analysis, Br. J. Radiol. 85 (2012) 1–10.
[3] C.A. Sullivan, S.E. Kahn, W.Y. Fujimoto, T. Hayashi, D.L. Leonetti, E.J. Boyko, Change in intra-abdominal fat predicts the risk of hypertension in Japanese Americans, Hypertension 66 (2015) 134–140.
[4] R. Bouchi, T. Takeuchi, M. Akihisa, N. Ohara, Y. Nakano, R. Nishitani, M. Murakami, T. Fukuda, M. Fujita, I. Minami, H. Izumiyama, K. Hashimoto, T. Yoshimoto, High visceral fat with low subcutaneous fat accumulation as a determinant of atherosclerosis in patients with type 2 diabetes, Cardiovasc. Diabetol. 14 (2015) 136.
[5] B.L. Wajchenberg, Subcutaneous and visceral adipose tissue: their relation to the metabolic syndrome, Endocr. Rev. 21 (2000) 697–739.
[6] A. Tchernof, J.P. Després, Pathophysiology of human visceral obesity: an update, Physiol. Rev. 93 (2013) 359–404.
[7] H.F. Lopes, M.L. Corrêa-Giannella, F.M. Consolim-Colombo, B.M. Egan, Visceral adiposity syndrome, Diabetol. Metab. Syndr. 8 (2016) 40.
[8] D.V. Schapira, R.A. Clark, P.A. Wolff, A.R. Jarrett, N.B. Kumar, N.M. Aziz, Visceral obesity and breast cancer risk, Cancer 74 (1994) 632–639.
[9] K.K. Mauland, Ø. Eng, S. Ytre-Hauge, I.L. Tangen, A. Berg, H.B. Salvesen, Ø. Salvesen, C. Krakstad, J. Trovik, E.A. Hoivik, H.M.J. Werner, G. Mellgren, I.S. Haldorsen, High visceral fat percentage is associated with poor outcome in endometrial cancer, Oncotarget 8 (2017) 105184–105195.
[10] G.R. Hunter, B.A. Gower, B.L. Kane, Age related shift in visceral fat, Int. J. Body Compos. Res. 8 (2010) 103–108.
[11] V. Svehliková, R.N. Bennett, F.A. Mellon, P.W. Needs, S. Piacente, P.A. Kroon, Y. Bao, Isolation, identification and stability of acylated derivatives of apigenin 7-O-glucoside from chamomile (Chamomilla recutita [L.] Rauschert), Phytochemistry 65 (2004) 2323–2332.
[12] L. Bevilacqua, F. Buiarelli, F. Coccioli, R. Jasionowska, Identification of compounds in wine by HPLC-tandem mass spectrometry, Ann. Chim. 94 (2004) 679–689.
[13] D. Patel, S. Shukla, S. Gupta, Apigenin and cancer chemoprevention: progress, potential and promise (review), Int. J. Oncol. 30 (2007) 233–245.
[14] X. Yan, M. Qi, P. Li, Y. Zhan, H. Shao, Apigenin in cancer therapy: anti-cancer effects and mechanisms of action, Cell Biosci. 7 (2017) 50.
[15] S. Panda, A. Kar, Apigenin (4',5,7-trihydroxyflavone) regulates hyperglycaemia, thyroid dysfunction and lipid peroxidation in alloxan-induceddiabetic mice, J. Pharm. Pharmacol. 59 (2007) 1543–1548.
[16] A.P. Rauter, A. Martins, C. Borges, H. Mota-Filipe, R. Pinto, B. Sepodes, J. Justino, Antihyperglycaemic and protective effects of flavonoids on streptozotocin-induced diabetic rats, Phytother. Res. 24 (2010) S133–S138.
[17] M. Ono, K. Fujimori, Antiadipogenic effect of dietary apigenin through activation of AMPK in 3T3-L1 cells, J. Agric. Food Chem. 59 (2011) 13346–13352.
[18] S.J. Priceman, M. Kujawski, S. Shen, G.A. Cherryholmes, H. Lee, C. Zhang, L. Kruper, J. Mortimer, R. Jove, A.D. Riggs, H. Yu, Regulation of adipose tissue T cell subsets by Stat3 is crucial for diet-induced obesity and insulin resistance, Proc. Natl. Acad. Sci. U.S.A. 110 (2013) 13079–13084.
[19] I.O. Vroegrijk, J.B. van Klinken, J.A. van Diepen, S.A. van den Berg, M. Febbraio, L.K. Steinbusch, J.F. Glatz, L.M. Havekes, P.J. Voshol, P.C. Rensen, K.W. van Dijk, V. van Harmelen, CD36 is important for adipocyte recruitment and affects lipolysis, Obesity Silver Spring (Silver Spring) 21 (2013) 2037–2045.
[20] M. Liu, P. Tso, S.C. Woods, Receptor CD36 links a risk-associated allele to obesity

and metabolic disorders, J. Biol. Chem. 293 (2018) 13349–13350.
[21] H.Y. Kwan, J.H. Wu, T. Su, X.J. Chao, B. Liu, X.Q. Fu, C.L. Chan, R.H.Y. Lau, A.K.W. Tse, Q.B. Han, W.F. Fong, Z.L. Yu, Cinnamon induces browning in subcutaneous adipocytes, Sci. Rep. 7 (2017) 247.
[22] C.S. Hudak, O. Gulyaeva, Y. Wang, S.M. Park, L. Lee, C. Kang, H.S. Sul, Pref-1 marks very early mesenchymal precursors required for adipose tissue development and expansion, Cell Rep. 8 (2014) 678–687.
[23] N.G. Sabbagha, H.J. Kao, C.F. Yang, C.C. Huang, W.D. Lin, F.J. Tsai, T.H. Chen, W.Y. Tarn, J.Y. Wu, Y.T. Chen, Alternative splicing in Acad8 resulting a mitochondrial defect and progressive hepatic steatosis in mice, Pediatr. Res. 70 (2011) 31–36.
[24] P. Gade, S.K. Roy, H. Li, S.C. Nallar, D.V. Kalvakolanu, Critical role for transcription factor C/EBP-beta in regulating the expression of death-associated protein kinase 1, Mol. Cell Biol. 28 (2008) 2528–2548.
[25] H.Y. Kwan, J.H. Wu, T. Su, X.J. Chao, H. Yu, B. Liu, X.Q. Fu, A.K.W. Tse, C.L. Chan, W.F. Fong, Z.L. Yu, Schisandrin B regulates lipid metabolism in subcutaneous adipocytes, Sci. Rep. 7 (2017) 10266.
[26] L. Qiao, C. Zou, P. Shao, J. Schaack, P.F. Johnson, J. Shao, Transcriptional regulation of fatty acid translocase/CD36 expression by CCAAT/enhancer-binding protein alpha, J. Biol. Chem. 283 (2008) 8788–8795.
[27] H.Y. Kwan, Y.M. Hu, C.L. Chan, H.H. Cao, C.Y. Cheng, S.Y. Pan, K.W. Tse, Y.C. Wu, Z.L. Yu, W.F. Fong, Lipidomics identification of metabolic biomarkers in chemically induced hypertriglyceridemic mice, J. Proteome. Res. 12 (2013) 1387–1398.
[28] J. Dai, K. Liang, S. Zhao, W. Jia, Y. Liu, H. Wu, Y. Lv, C. Cao, T. Chen, S. Zhuang, X. Hou, S. Zhou, X. Zhang, X.W. Chen, Y. Huang, R.P. Xiao, Y. Wang, T. Luo, J. Xiao, C. Wang, Chemoproteomics reveals baicalin activates hepatic CPT1 to ameliorate diet-induced obesity and hepatic steatosis, Proc. Natl. Acad. Sci. U.S.A. 115 (2018) E5896–5905.
[29] A.J. Richard, J.M. Stephen, The role of JAK-STAT signalling in adipose tissue function, Biochim. Biophys. Acta. 1842 (2014) 431–439.
[30] S.D. Hursting, M.J. Hursting, Growth signals, inflammation, and vascular perturbations: mechanistic links between obesity, metabolic syndrome and cancer, Arterioscler. Thromb. Vasc. Biol. 32 (2012) 1766–1770.
[31] R. Jafari, H. Almqvist, H. Axelsson, M. Ignatushchenko, T. Lundbäck, P. Nordlund, D. Martinez Molina, The cellular thermal shift assay for evaluating drug target interactions in cells, Natl. Protoc. 9 (2014) 2100–2122.
[32] U. Rozovski, D.M. Harris, P. Li, Z. Liu, P. Jain, A. Ferrajoli, J. Burger, P. Thompson, N. Jain, W. Wierda, M.J. Keating, Z. Estrov, STAT3-activated CD36 facilitates fatty acid uptake in chronic lymphocytic leukemia cells, Oncotarget 9 (2018) 21268–21280.
[33] A.G. Jay, J.A. Hamilton, The enigmatic membrane fatty acid transporter CD36: new insights into fatty acid binding and their effects on uptake of oxidized LDL, Prostaglandins Leukot. Essent. Fatty Acids 138 (2018) 64–70.
[34] J.B. Harp, D. Franklin, A.A. Vanderpuije, J.M. Gimble, Differential expression of signal transducers and activators of transcription during human adipogenesis, Biochem. Bioiphys. Res. Commun. 281 (2001) 907–912.
[35] D. Wang, Y. Zhou, W. Lei, K. Zhang, J. Shi, Y. Hu, G. Shu, J. Song, Signal transducer and activator of transcription 3 (STAT3) regulates adipocyte differentiation via peroxisome-proliferator-activated receptor gamma (PPARgamma), Biol. Cell 102 (2009) 1–12.
[36] J. Yang, K.W. Park, S. Cho, Inhibition of the CD36 receptor reduces visceral fat accumulation and improves insulin resistance in obese mice carrying the BDNF-Val66Met variant, J. Biol. Chem. 293 (2018) 13338–13348.
[37] V. Christiaens, M. Van Hul, H.R. Lijnen, I. Scroyen, CD36 promotes adipocyte differentiation and adipogenesis, Biochim. Biophys. Acta. 1820 (2012) 949–956.
[38] M. Liu, P. Tso, S.C. Woods, Receptor CD36 links a risk-associated allele to obesity and metabolic disorders, J. Biol. Chem. 293 (2018) 13349–13350.
[39] P. Fiorina, M. Lanfredini, A. Montanari, M.G. Peca, A. Veronelli, A. Mello, E. Astorri, A. Craveri, Plasma homocysteine and folate are related to arterial blood pressure in type 2 diabetes mellitus, Am. J. Hypertens. 11 (1998) 1100–1107.
[40] Y. Feng, M.Q. Shan, L. Bo, X.Y. Zhang, J. Hu, Association of homocysteine with type 1 diabetes mellitus: a meta-analysis, Int. J. Clin. Exp. Med. 8 (2015) 12529–12538.
[41] R.J. Stratta, Cardiovascular disease and neoplasms after pancreas transplantation, Lancet 352 (1998) 65–66.
[42] R.F. Saidi, Current status of pancreas and islet cell transplantation, Int. J. Organ Transplant. Med. 3 (2012) 54–60.
[43] X. Feng, W. Yu, X. Li, F. Zhou, W. Zhang, Q. Shen, J. Li, C. Zhang, S.P. Apigenin, a modulator of PPARγ, attenuates HFD-induced NAFLD by regulating hepatocyte lipid metabolism and oxidative stress via Nrf2 activation, Biochem. Pharmacol. 136 (2017) 136–149.
[44] X. Feng, D. Weng, F. Zhou, Y.D. Owen, H. Qin, J. Zhao, Huang Y. WenYu, J. Chen, H. Fu, N. Yang, D. Chen, J. Li, R. Tan, P. Shen, Activation of PPARγ by a natural flavonoid modulator, apigenin ameliorates obesity-related inflammation via regulation of macrophage polarization, EBioMedicine 9 (2016) 61–76.
[45] L. Maréchal, M. Laviolette, A. Rodrigue-Way, B. Sow, M. Brochu, V. Caron, A. Tremblay, The CD36-PPARγ pathway in metabolic disorders, Int. J. Mol. Sci. 19 (2018) 1529.
[46] H.J. Lim, S. Lee, K.S. Lee, J.H. Park, Y. Jang, E.J. Lee, H.Y. Park, PPAR gamma activation induces CD36 expression and stimulates foam cell like changes in rVSMCs, Prostaglandins Other Lipid Mediat. 80 (2006) 165–174.
[47] L. Hanske, G. Loh, S. Sczesny, M. Blaut, A. Braune, The bioavailability of apigenin-7-glucoside is influenced by human intestinal microbiota in rats, J. Nutr. 139 (2009) 1095–1102.
[48] K.A. Khaled, Y.M. El-Sayed, B.M. Al-Hadiya, Disposition of the flavonoid quercetin in rats after single intravenous and oral doses, Drug Dev. Ind. Pharm. 29 (2003) 397–403.
[49] J. Liang, W. Wu, Q. Liu, S. Chen, Long-circulating nanoliposomes (LCNs) sustained delivery of baicalein (BAI) with desired oral bioavailability in vivo, Drug Deliv. 20 (2013) 319–323.
[50] T. Chen, L.P. Li, X.Y. Lu, H.D. Jiang, S. Zeng, Absorption and excretion of luteolin and apigenin in rats after oral administration of Chrysanthemum morifolium extract, J. Agric. Food Chem. 55 (2007) 273–277.
[51] L. Hanske, G. Loh, S. Sczesny, M. Blaut, A. Braune, The bioavailability of apigenin-7-glucoside is influenced by human intestinal microbiota in rats, J. Nutr. 39 (2009) 1095–1102.
[52] D. Tang, K. Chen, L. Huang, J. Li, Pharmacokinetic properties and drug interactions of apigenin, a natural flavone, Expert Opin. Drug Metab. Toxicol. 13 (2017) 323–330.
[53] B. Mafuvadze, Y. Liang, C. Besch-Williford, X. Zhang, S.M. Hyder, Apigenin induces apoptosis and blocks growth of medroxyprogesterone acetate-dependent BT-474 xenograft tumors, Horm. Cancer 3 (2012) 160–171.
[54] B. Sung, H.Y. Chung, N.D. Kim, Role of apigenin in cancer prevention via the induction of apoptosis and autophagy, J. Cancer Prev. 21 (2016) 216–226.